NMR crystallography of campho[2,3-c]pyrazole (Z' = 6): Combining high-resolution 1H-13C solid-state MAS NMR spectroscopy and GIPAW chemical-shift calculations

ARTICLE *in* THE JOURNAL OF PHYSICAL CHEMISTRY A · SEPTEMBER 2010

Impact Factor: 2.69 · DOI: 10.1021/jp104901j · Source: PubMed

4 AUTHORS, INCLUDING:

Rosa M Claramunt
National Distance Education University
472 PUBLICATIONS **5,608** CITATIONS

SEE PROFILE

NMR Crystallography of Campho[2,3-c]pyrazole ($Z' = 6$): Combining High-Resolution ^{1}H-^{13}C Solid-State MAS NMR Spectroscopy and GIPAW Chemical-Shift Calculations

Amy L. Webber,[†] Lyndon Emsley,[‡] Rosa M. Claramunt,[§] and Steven P. Brown*[,†]

Department of Physics, University of Warwick, Coventry CV4 7AL, U.K., Université de Lyon, Centre de RMN à très hauts champs, CNRS/ENS Lyon/UCBL, 5 rue de la Doua, 69100 Villeurbanne, France, and Departamento de Química Orgánica y Bio-Orgánica, Facultad de Ciencias, UNED, Senda del Rey 9, E-28040 Madrid, Spain

Received: May 28, 2010; Revised Manuscript Received: August 5, 2010

^{1}H-^{13}C two-dimensional magic-angle spinning (MAS) solid-state NMR correlation spectra, recorded with the MAS-*J*-HMQC experiment, are presented for campho[2,3-c]pyrazole. For each ^{13}C moiety, there are six resonances associated with the six distinct molecules in the asymmetric unit cell ($Z' = 6$). The one-bond C−H correlations observed in the 2D ^{1}H-^{13}C MAS-*J*-HMQC spectra allow the experimental determination of the ^{1}H and ^{13}C chemical shifts associated with the separate CH, CH_2, and CH_3 groups. ^{1}H and ^{13}C chemical shifts calculated by using the GIPAW (Gauge Including Projector Augmented Waves) plane-wave pseudopotential approach are presented. Calculations for the whole unit cell ($12 \times 29 = 348$ atoms, with geometry optimization of all atoms) allow the assignment of the experimental ^{1}H and ^{13}C chemical shifts to the six distinct molecules. The calculated chemical shifts for the full crystal structure are compared with those for isolated molecules as extracted from the geometry-optimized crystal structure. In this way, the effect of intermolecular interactions on the observed chemical shifts is quantified. In particular, the calculations are sufficiently precise to differentiate the small (<1 ppm) differences between the ^{1}H chemical shifts of the six resonances associated with each distinct CH or CH_2 moiety.

1. Introduction

There is increasing interest in crystal structures with more than one independent molecule in the asymmetric unit cell ($Z' > 1$).[1−9] ^{13}C cross-polarization (CP) magic-angle spinning (MAS) NMR is a routine method for unambiguously determining Z' by means of comparing the number of observed resonances with the number of chemically distinct carbon atoms in the molecule.[10] The assignment of the observed ^{13}C solid-state NMR resonances to the distinct molecules in the asymmetric unit cell is, however, a considerable challenge.

This paper shows that the $6 \times 11 = 66$ ^{13}C resonances for the six independent molecules of campho[2,3-c]pyrazole can be assigned by means of experimental ^{1}H-^{13}C MAS-*J*-HMQC[11] two-dimensional (2D) solid-state NMR spectra and GIPAW (Gauge Including Projector Augmented Waves) chemical-shift calculations.[12,13] Experimentally, the determination of correlated ^{13}C and ^{1}H chemical shifts for the directly bonded CH, CH_2, or CH_3 moieties relies upon, first, high resolution in the ^{1}H dimension that can be achieved by means of ^{1}H homonuclear decoupling methods[14] such as the frequency-switched and phase-modulated Lee−Goldburg (FSLG[15] and PMLG[16]) and DUMBO[17−20] sequences and, second, coherence transfer between ^{13}C and ^{1}H via through-bond $^{1}J_{CH}$ couplings.[11,21] Notably, the approach here is built upon the sensitivity of the ^{1}H chemical shift to intermolecular interactions, namely, aromatic $\pi-\pi$ interactions and hydrogen bonding,[22−24] and relies upon the demonstrated power of the GIPAW approach for calculating NMR properties for full periodic crystal structures, specifically in this context of organic solids.[25−36] This study further shows that quantitative insight into the effect of intermolecular interactions on NMR chemical shifts is obtained by comparing calculations for the full crystal structure with those for isolated molecules.

2. Experimental Methods

2.1. Sample Preparation and Solid-State NMR. Campho[2,3-c]pyrazole, **1**, was synthesized from natural camphor by using the procedure described in ref 37. The carbon atoms are numbered according to Table 5 of ref 38; note that this numbering is different from that in ref 39.

Spectra were recorded on a Bruker DSX spectrometer, operating at ^{1}H and ^{13}C Larmor frequencies of 500.1 and 125.8 MHz, respectively. For all ^{13}C detected experiments, a Bruker 4 mm triple-resonance probe (operating in double-resonance mode) was used at a MAS frequency of 12.5 kHz, with a ^{1}H nutation frequency of 100 kHz. ^{13}C magnetization was created by ramped cross-polarization[40,41] (100−50%), and heteronuclear ^{1}H TPPM[42] decoupling with a 15° phase increment and 4.6 μs pulses (4.8 μs for MAS-*J*-HMQC) was applied during a t_2 acquisition time of 40 ms.

^{1}H-^{13}C MAS-J-HMQC.[11] A CP contact pulse of 2 ms duration was used, and the ^{13}C 180° pulse was of duration 7.4 μs. Homonuclear ^{1}H decoupling was achieved during the *J* evolution periods, τ and t_1, by using the FSLG[15] technique, with cycled blocks of 16 μs and magic pulses of 1.52 μs. A nested 16-step phase cycle was used to select $\Delta p = \pm 1$ on the first (before CP, 2 steps) and second (before t_1, 2 steps) ^{1}H 90° pulses and $\Delta p = \pm 2$ on the ^{13}C 180° pulse (4 steps), where p is the coherence order; see Figure 1 of ref 11 for a pulse sequence and coherence transfer pathway diagram. Sign discrimination was achieved in the indirect dimension by the STATES method; 400 separate t_1 FIDs were acquired with an increment of 64 μs,

* Corresponding author. E-mail: S.P.Brown@warwick.ac.uk.
[†] University of Warwick.
[‡] CNRS/ENS Lyon/UCBL.
[§] Facultad de Ciencias, UNED.

10.1021/jp104901j
Published on Web 09/03/2010

that is, corresponding to a total t_1 acquisition time of 12.8 ms. For the two spectra with $\tau = 2.384$ and 0.928 ms, 32 and 112 transients were coadded, with recycle delays of 4.5 and 5.2 s, corresponding to experimental times of 16 and 65 h, respectively. The ^{1}H chemical-shift axis was calibrated (a scaling factor of 0.62 was used) such that the mean CH_3 (H8, H10, H11) and aromatic CH (H1) ^{1}H chemical shifts equal 0.6 and 7.0 ppm, respectively, corresponding to the single-quantum (SQ) frequencies observed under fast (30 kHz) MAS in a ^{1}H double-quantum (DQ) MAS (see below) spectrum. Quoted experimental ^{1}H chemical shifts are accurate to ±0.2 ppm.

^{1}H DQ MAS:[43] The experiment was performed by using a Bruker 2.5 mm probe at a MAS frequency of 30 kHz, with a ^{1}H 90° pulse duration of 2 μs. One rotor period of the back-to-back (BABA)[44,45] recoupling sequence ($90_x-\tau-90_{-x}-90_y-\tau-90_{-y}$, where $\tau = \tau_R/2$ minus the pulse durations) was used for excitation and reconversion of DQ coherence. For each of 64 separate t_1 FIDs (by using the States-TPPI method with a rotor-synchronized increment of 33.3 μs), 16 transients were coadded with a recycle delay of 3 s. A 16-step phase cycle was used to select $\Delta p = \pm 2$ on the DQ excitation pulses (4 steps) and $\Delta p = -1$ (4 steps) on the z-filter 90° pulse.

1

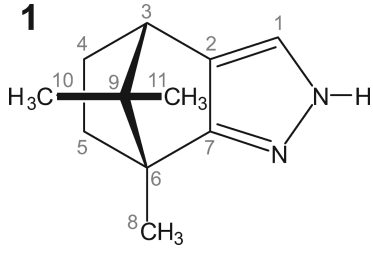

2.2. First-Principles NMR Chemical-Shift Calculations. First-principles calculations were performed by using the academic release version 4.3 of the CASTEP[46] software package, which implements density functional theory (DFT) within a generalized gradient approximation and the planewave pseudopotential approach. All calculations used the PBE exchange-correlation functional[47] and ultrasoft pseudopotentials.[48]

Geometry optimization was performed by starting with the X-ray diffraction crystal structure of campho[2,3-c]pyrazole (obtained from the CSD database, refcode LABHEB,[38] $R = 0.059$ for 5489 observed reflections). A comparison of the average forces remaining on the atoms after geometry optimization was carried out for proton-only and all-atom optimizations by using a maximum planewave cutoff energy of 600 eV. When constrained, the heavy atoms were still affected by average forces (given as Cartesian components) of 0.315 and 0.402 eV/Å for carbon and nitrogen, respectively, as compared to 0.005 eV/Å for the protons, indicating that further relaxation of the heavy atoms was necessary. Where all atoms were relaxed, the average forces were determined to be of a similar magnitude for all atomic species, that is, 0.010 (C), 0.016 (N), and 0.009 (H) eV/Å. Hence, an all-atom relaxed structure was used for NMR chemical-shift calculations, performing the geometry optimization with a maximum planewave cutoff energy of 800 eV. Note that distances stated in this paper are for this geometry-optimized crystal structure: when comparing the database crystal structure with the geometrically optimized structure, the root mean squared deviation was 0.043 Å for heavy atoms (carbon and nitrogen) and 0.244 Å for hydrogen, corresponding to 0.183 Å for all atoms.

The NMR chemical shifts were computed by using the gauge-including projector augmented-wave (GIPAW) method.[12,13] The calculations upon the full crystal structure used a planewave basis set with a maximum cutoff energy of 1000 eV, with integrals taken over the Brillouin zone by using a Monkhorst-Pack grid of minimum sample spacing 0.08 A^{-1}. Calculation of the shielding tensors for all nuclei in the full crystal took 27 h real time, using 32 nodes and 125 GB RAM on the University of Warwick Centre for Scientific Computing cluster of 3 GHz Intel Xeon 5160 processors.

In order to compare directly with experimentally measured isotropic chemical shifts, the following expression is used:

$$\delta_{iso} = -[\sigma_{iso} - \sigma_{ref}] \quad (1)$$

where σ_{iso} is the absolute isotropic shielding value generated from the first-principles calculation. The standard practice[25] is that σ_{ref} is chosen for each nucleus such that the means of the calculated and experimental chemical shifts coincide. This procedure gives σ_{ref} (^{13}C) = 172.2 ppm and σ_{ref} (^{1}H) = 30.7 ppm (chemical-shift values determined by using these universal referencing values can be found in the Supporting Information); however (as discussed in Section 3.2), the local agreement with respect to experiment for each chemically distinct atom was much better if these referencing values were adjusted for separate atoms of the molecule. The individual referencing values used are in the range σ_{ref} (^{13}C) = 166.3−173.2 ppm and σ_{ref} (^{1}H) = 29.2−30.9 ppm and are listed in Tables 1−3 and S3 and S4 in the Supporting Information.

Calculations were also performed upon each of the six independent molecules of the asymmetric unit cell, that is, in an isolated environment. For these, one complete molecule was extracted and placed into a cubic supercell of dimensions 10 × 10 × 10 Å^3, where simple cubic (P1) periodicity was reintroduced. NMR chemical-shielding values were computed for the three separate instances whereby the isolated structure was (i) not further optimized, (ii) optimized with all atoms allowed to relax, (iii) optimized with only the hydrogen atoms allowed to relax (values resulting from the first of these three calculations are presented in the main text, and the chemical shifts computed for optimized isolated molecules are presented in the Supporting Information). For each of these three cases, all geometry optimizations and NMR shielding calculations used a planewave basis set with a maximum energy of 1000 eV, with integrals taken over the Brillouin zone by using a minimum sample spacing 0.05 A^{-1}. A 10 × 10 × 10 Å^3 supercell was used because, in test calculations for supercells of dimension 6, 7, 8, 9, and 10 Å^3, it was found that the chemical-shift values had converged to within 0.1 and 0.2 ppm for ^{1}H and ^{13}C, respectively. Calculations of the shielding tensors for nuclei in the isolated molecules took up to 9 h real time when using eight nodes and 32 GB RAM. Chemical shifts calculated for the isolated molecules are referenced by using the individual chemical-moiety reference shieldings as determined for the full crystal structure.

3. Results

3.1. ^{13}C CP MAS Spectrum. In the solid state, campho[2,3-c]-pyrazole crystallizes with six independent molecules in the asymmetric unit cell by the formation of two cyclic trimers,[38] as is shown for the geometry-optimized crystal structure in Figure 1a. A ^{13}C CP MAS spectrum is shown in Figure 1b, with the ^{13}C spectral regions assigned on the basis of previous solution− and solid−state NMR studies.[38,39] The variations in

TABLE 1: Experimental and Calculated (GIPAW) ^{13}C and ^{1}H Chemical Shifts of CH and CH_3 Groups of Campho[2,3-c]pyrazole

expt[a] /ppm			calculated[b]/ppm			
^{13}C	^{1}H		^{13}C		^{1}H	
		molecule	cryst[c]	mol[d]	cryst[c]	mol[d]
C1	H1					
122.2	7.4	**C**	122.2	115.1	7.0	6.5
121.5	7.0	**A**	121.3	115.0	7.0	6.5
120.5	6.6	**F**	120.4	114.8	6.5	6.5
118.8	6.9	**E**	118.9	115.5	7.0	6.5
118.8	6.9	**B**	118.8	115.1	7.0	6.6
118.8	7.0	**D**	118.3	115.3	7.1	6.6
C3	H3					
48.2	2.5	**A**	47.8	47.5	2.5	2.3
48.1	2.1	**C**	48.1	47.8	1.9	2.3
47.4	2.6	**B**	47.2	47.5	2.5	2.3
47.4	1.9	**D**	47.8	48.2	2.0	2.3
46.9	2.7	**F**	46.8	47.4	2.7	2.1
46.9	2.5	**E**	47.1	47.2	2.6	2.2
C11	H11 a−c[e]					
23.4	0.2	**E**	23.6	17.6	0.2	0.1
21.3	0.0	**B**	22.0	17.4	−0.1	0.4
21.3	0.0	**F**	21.2	18.3	0.0	0.3
20.2	0.3	**A**	19.9	17.6	0.3	0.1
20.2	0.3	**C**	19.3	16.6	0.6	0.2
20.0	−0.2	**D**	20.2	17.7	−0.1	0.4
C10	H10 a−c[e]					
21.3	0.4	**B**	21.8	17.6	0.4	0.6
20.9	0.3	**E**	21.1	17.2	0.6	0.5
20.9	−0.3	**D**	20.5	17.7	−0.3	0.6
20.7	0.4	**F**	20.5	17.6	0.4	0.6
18.9	0.3	**C**	19.1	17.0	0.5	0.5
18.2	−0.2	**A**	17.8	17.0	−0.2	0.5
C8	H8 a−c[e]					
13.0	1.2	**C**	13.0	7.5	1.4	0.7
12.1	1.1	**F**	12.6	8.0	1.4	0.8
12.0	0.5	**A**	12.2	7.8	0.4	0.7
11.8	0.6	**D**	12.1	7.7	0.7	0.8
10.8	0.8	**B**	10.3	7.3	0.7	0.8
10.1	0.2	**E**	9.5	7.4	0.0	0.7

[a] As determined from the ^{1}H-^{13}C MAS-*J*-HMQC ($\tau = 2.4$ ms) spectrum in Figure 2a. [b] Calculated chemical-shift references (σ_{ref}) were determined separately for each chemically distinct CH and CH_3 group: σ_{ref} (^{13}C)/ppm = 170.0 (C1), 169.3 (C3), 172.9 (C11), 173.2 (C10), 173.2 (C8); σ_{ref} (^{1}H)/ppm = 29.9 (H1), 30.4 (H3), 30.7 (H11a−c), 30.6 (H10a−c), 30.7 (H8a−c). [c] Calculation for full crystal structure, geometry-optimized with all atoms allowed to relax. [d] Calculation for isolated molecule extracted from geometry-optimized full crystal. [e] Average calculated ^{1}H chemical shift over the three CH_3 protons.

TABLE 2: Experimental and Calculated (GIPAW) ^{13}C and ^{1}H Chemical Shifts of CH_2 Groups of Campho[2,3-c]pyrazole

expt[a] /ppm			calculated[b]/ppm			
^{13}C	^{1}H		^{13}C		^{1}H	
			cryst[c]	mol[d]	cryst[c]	mol[d]
C5	H5 a,b					
36.2	0.5	**D**	36.5	33.7	0.4	0.5
	0.7				0.7	1.1
35.3	0.7	**B**	35.3	32.4	0.8	0.1
	1.6				1.9	−0.2
34.9	1.3	**C**	35.0	33.0	1.4	−0.4
	1.6				2.0	−0.2
33.6	1.2	**F**	33.3	32.8	1.0	0.0
	1.8				1.5	0.3
33.2	1.4	**A**	32.5	32.6	1.5	−0.4
	1.6				1.5	0.4
32.2	0.9	**E**	31.2	32.1	0.7	0.4
	1.1				1.0	0.9
C4	H4 a,b					
29.7	0.9	**B**	29.7	27.4	1.1	−0.4
	1.5				2.0	−0.1
28.9	0.4	**D**	28.1	26.7	0.6	0.2
	1.9				1.5	0.3
28.7	1.6	**C**	28.7	26.3	1.6	−0.7
	2.4				2.2	−0.3
28.6	0.9	**E**	27.9	26.4	1.0	0.0
	2.3				2.0	−0.1
28.2	1.1	**A**	27.9	26.2	0.9	0.1
	1.5				1.6	0.4
27.4	0.6	**F**	27.4	26.8	0.6	0.3
	0.7				0.7	1.2

[a] As determined from the ^{13}C CP MAS spectrum in Figure 1b and the ^{1}H-^{13}C MAS-*J*-HMQC ($\tau = 0.9$ ms) spectrum in Figure 2b. [b] Calculated chemical-shift references (σ_{ref}) were determined separately for each chemically distinct CH_2 ^{13}C and the attached protons: σ_{ref} (^{13}C)/ppm = 167.9 (C5), 171.6 (C4). σ_{ref} (^{1}H)/ppm = 30.8 (H5a), 30.5 (H5b), 30.9 (H4a), 30.8 (H4b). [c] Calculation for full crystal structure, geometry-optimized with all atoms allowed to relax. [d] Calculation for isolated molecule extracted from geometry-optimized full crystal.

chemical environment for each of these independent molecules gives rise to an evident multiplicity of resonances; for example, see the six resolved resonances for C5 in the expanded region (expanded regions for all resonances of the ^{13}C CP MAS spectrum are shown in Figures S1 and S2 in the Supporting Information).

3.2. ^{1}H-^{13}C MAS-*J*-HMQC Spectra and GIPAW Full-Crystal Calculations. Figure 2 presents high-resolution ^{1}H-^{13}C correlation spectra of campho[2,3-c]pyrazole, recorded by using the MAS-*J*-HMQC[11] sequence and FSLG[15] ^{1}H homonuclear decoupling. As compared to dipolar-mediated heteronuclear correlation methods, this experiment uses heteronuclear multiple-quantum coherence (HMQC) generated by scalar couplings to establish correlations between resonances due to bonded pairs of carbon and hydrogen nuclei. Furthermore, the use of a short evolution period, τ, ensures that the experiment is selective for directly bonded carbon and hydrogen atoms. Two ^{1}H-^{13}C MAS-*J*-HMQC spectra are shown in Figure 2, corresponding to (a) $\tau = 2.4$ ms and (b) $\tau = 0.9$ ms. The former case (a) gives optimized peak intensity for CH and CH_3 resonances, whereas faster dephasing is observed for CH_2 groups, such that the magnetization transfer for CH_2 groups is optimal at the shorter τ of 0.9 ms in (b).

The six areas highlighted in gray in Figure 2 are expanded in Figure 3, corresponding to the chemical shift regions of the protonated carbon atoms, specifically, (a) and (b) CH (C1 and C3), (c) and (d) CH_3 (C10, C11, and C8);, and (e) and (f) CH_2 (C5 and C4) resonances. In addition to the spread of ^{13}C resonances for each distinct carbon, a spread of the ^{1}H resonances of the directly attached protons is observed. Although the range of experimental ^{1}H chemical shifts within a group of resonances is small (up to 1 ppm for the CH and CH_3 groups), the narrow linewidths (e.g., full width at half-maximum height (FWHMH) equals 0.3 ppm (170 Hz) for the resolved H1 CH resonances) in the high-resolution ^{1}H dimension allows the resolution of distinct 2D ^{1}H-^{13}C resonances that otherwise overlap in the 1D ^{13}C CP MAS spectrum. For example, consider the crowded region between 20 and 22 ppm in the ^{13}C dimension due to the C10 and C11 CH_3 groups: in the 2D spectrum in Figure 3c, six peaks can be identified as compared to three peaks and a shoulder in the ^{13}C CP MAS spectrum (see Figure S1c in the Supporting Information).

TABLE 3: Experimental and Calculated (GIPAW) ^{13}C Chemical Shifts of Non-Protonated Carbons of Campho[2,3-c]pyrazole

expt[a] /ppm	molecule	calculated[b]/ppm	
^{13}C		^{13}C	
		cryst[c]	mol[d]
	C7		
166.9	**A**	167.2	166.3
166.1	**B**	166.2	165.5
165.5	**E**	165.4	165.7
165.3	**F**	165.1	165.2
165.2	**D**	165.0	164.9
165.0	**C**	164.7	165.5
	C2		
126.3	**D**	126.7	124.4
125.6	**E**	125.6	124.7
125.4	**A**	125.5	124.2
125.3	**F**	125.3	124.3
125.0	**B**	125.0	123.7
124.9	**C**	124.7	123.9
	C9		
62.9	**E**	63.2	59.5
62.4	**F**	62.5	59.7
62.2	**A**	62.4	59.9
61.6	**C**	61.5	58.9
61.0	**D**	60.8	58.1
60.8	**B**	60.5	57.8
	C6		
51.0	**A**	51.2	49.6
50.8	**C**	50.4	48.7
50.6	**B**	50.3	48.9
50.4	**E**	50.3	49.3
49.8	**D**	49.6	49.1
49.7	**F**	49.5	49.5

[a] As determined from the ^{13}C CP MAS spectrum in Figure 1b. [b] Calculated chemical-shift references (σ_{ref}) were determined separately for each chemically distinct carbon atom: σ_{ref} (^{13}C)/ppm = 167.8 (C7), 166.5 (C2), 166.3 (C9), 167.9 (C6). [c] Calculation for full crystal structure, geometry-optimized with all atoms allowed to relax. [d] Calculation for isolated molecule extracted from geometry-optimized full crystal.

The experimental ^{13}C and ^{1}H chemical shifts as determined from the MAS-*J*-HMQC spectra as well as the ^{13}C CP MAS spectrum are presented in Tables 1 (CH and CH_3), 2 (CH_2), and 3 (quaternary C), together with chemical shifts as calculated (GIPAW) for the full periodic crystal structure. Crosses in Figure 3 indicate the ^{13}C and ^{1}H chemical shifts as calculated for the full crystal structure. A weakness of the DFT-based GIPAW method (and also quantum-chemical calculations based on the gauge-including atomic orbital (GIAO) method) is that calculated low- and high-ppm resonances are under- and overestimated as compared to experiment, such that the best-fit line to a plot of calculated chemical shift against experiment chemical shift has a gradient that deviates from unity.[25,34] In this work, we have referenced the calculated values by using reference shieldings, σ_{ref} (^{13}C) and σ_{ref} (^{1}H), that are separately determined for each individual set of six resonances associated with each chemically distinct carbon in the campho[2,3-c]pyrazole molecule. The use of separately determined reference shieldings here allows the direct comparison of experimental and calculated chemical shifts. (Calculated chemical shifts, as referenced by using the standard practice based upon a single universal reference shielding are presented in Table S1 in the Supporting Information.)

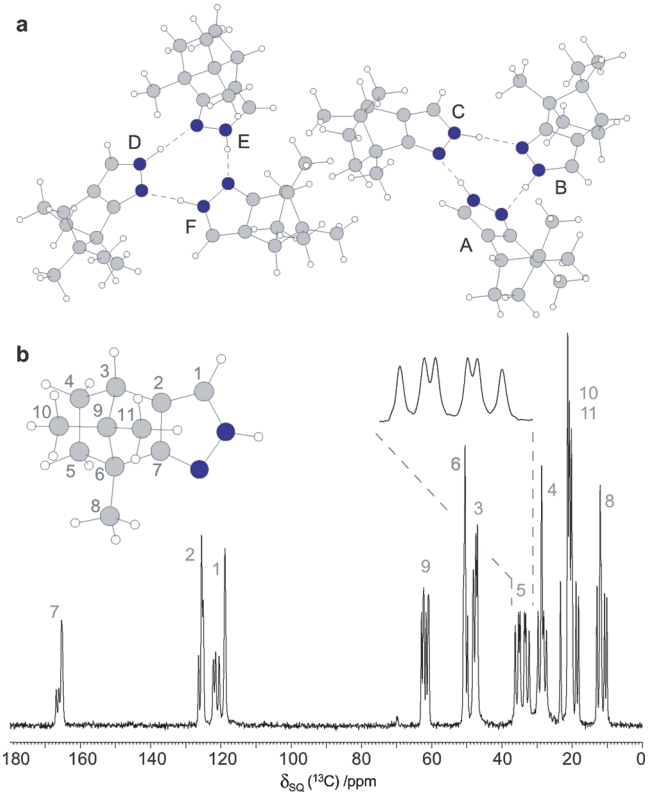

Figure 1. (a) Geometry-optimized (CASTEP) crystal structure of campho[2,3-c]pyrazole, where the organization of the six independent molecules in the asymmetric unit cell ($Z' = 6$) into two hydrogen-bonded trimers is evident.[38] (b) ^{13}C (125 MHz) CP MAS spectrum of campho[2,3-c]pyrazole recorded at 12.5 kHz MAS. The contact time was 1 ms, and 1024 transients were coadded with a recycle delay of 3 s. The peaks for the 11 distinct atoms are labeled as shown in the structure inset. The six resolved resonances for C5 are shown in an expanded region.

It is to be noted that a comparison is made here between experimental chemical shifts and calculations performed for a static structure at a temperature of absolute zero. In this context, small increases in experimental ^{1}H chemical shifts of hydrogen-bonded resonances have been observed upon decreasing temperature,[49−52] whereas calculations by Dumez and Pickard that consider the effect of vibrational averaging on calculated ^{1}H chemical shifts[53] (building on a previous study of the temperature dependence of ^{17}O and ^{25}Mg chemical shifts in solid MgO[54]) show an increase of 0.5 ppm when comparing the consideration of vibrational averaging at 293 and 0 K. Moreover, de Gortari et al. have shown that the agreement between calculation and experiment for ^{13}C chemical shifts in the MLP peptide is improved by considering the time averaging over vibrational and rotameric states that are found to be populated during first-principles and classical molecular-dynamics simulations.[55] Hansen et al. have also considered averaged chemical shifts on a picoseconds time scale in a perylene tetracarboxydiimide derivative.[56] Given the focus of this work on the CH, CH_2, and CH_3 groups in campho[2,3-c]pyrazole, a variable-temperature investigation is, however, beyond the scope of this article.

Figure 3 shows that there is good agreement between the calculated and experimental ^{13}C and ^{1}H chemical shifts of the directly bonded CH, CH_2, and CH_3 groups. Quantitatively, the mean absolute difference between experiment and calculation is 0.3 ppm (^{13}C: CH and CH_3 groups in Table 1), 0.1 ppm (^{1}H: CH and CH_3 groups in Table 1), 0.2 ppm (^{13}C: CH_2 groups in

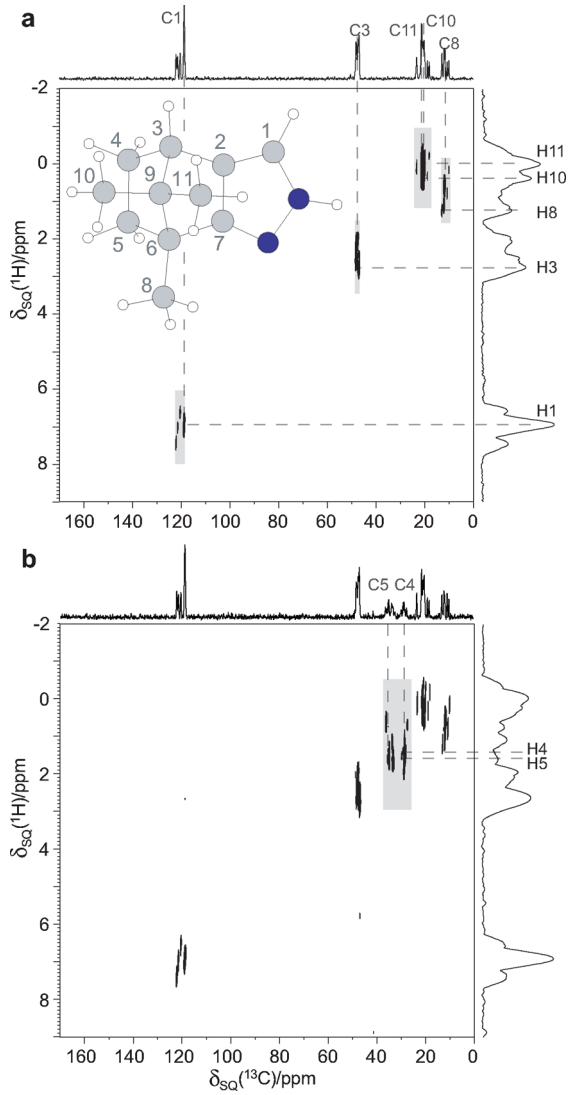

Figure 2. ^{1}H-^{13}C MAS-*J*-HMQC (with ^{1}H FSLG homonuclear decoupling) spectra, together with skyline projections, of campho[2,3-c]pyrazole recorded at a ^{1}H Larmor frequency of 500 MHz and 12.5 kHz MAS, obtained by using a τ evolution period of (a) 2.4 ms and (b) 0.9 ms. The base contour is at (a) 20% and (b) 18%. The highlighted areas are shown as expanded regions in Figure 3.

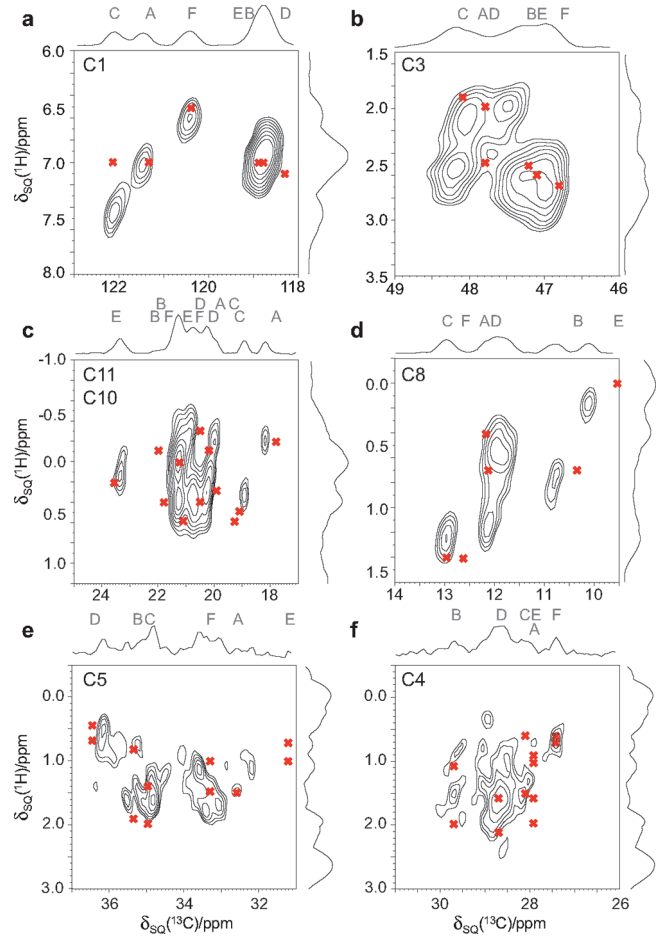

Figure 3. Expanded regions of the ^{1}H-^{13}C MAS-*J*-HMQC spectra shown in Figure 2 highlighting the ^{13}C and ^{1}H chemical shifts associated with the protonated carbon atoms of campho[2,3-c]pyrazole: taken from Figure 2a, CH (a) C1 and (b) C3, CH_3 (c) C10 and C11, and (d) C8; taken from Figure 2b, CH_2 (e) C5 and (f) C4. The base contour level is shown at (a−d) 23% and (e−f) 13%. Red crosses indicate the calculated (GIPAW) ^{1}H and ^{13}C chemical shifts, as determined by using the geometry-optimized (CASTEP) full crystal structure of campho-[2,3-c]pyrazole. Labels A−F correspond to the six distinct molecules in the asymmetric unit cell (see Figure 1a).

Table 2), 0.2 ppm (^{1}H: CH_2 groups in Table 2), and 0.2 ppm (^{13}C: quaternary C groups in Table 3). Moreover, the calculations reproduce very well the spread in both the ^{13}C and ^{1}H chemical shifts (see Table 4), with the calculated spreads agreeing with experiment to within 1.3 and 0.4 ppm for ^{13}C and ^{1}H, respectively. GIPAW chemical-shift calculations that show good agreement with the correlated ^{13}C and ^{1}H chemical shifts as determined from a 2D ^{13}C-^{1}H NMR spectrum have also been presented for penicillin[30] and the anhydrate form of terbutaline sulfate.[57] In conclusion, for campho[2,3-c]pyrazole, the 2D correlation of ^{13}C and ^{1}H chemical shifts via one-bond $^{1}J_{CH}$ couplings allows, in combination with the GIPAW chemical-shift calculations for the full crystal structure, an assignment of the resonances to the six distinct molecules in the asymmetric unit cell (see Tables 1 and 2).

3.3. ^{1}H DQ MAS Spectrum. A ^{1}H DQ MAS (30 kHz) spectrum of campho[2,3-c]pyrazole is shown in Figure 4a. It is evident that the resolution is much worse compared to that in the 2D ^{1}H-^{13}C MAS-*J*-HMQC spectra (Figure 2) recorded with ^{1}H FSLG decoupling. However, even if there is no resolution for the low-ppm aliphatic resonance, distinct NH and aromatic CH (H1) resonances are resolved, although it is not possible to identify separate resonances corresponding to the six distinct molecules in the asymmetric unit cell, as is possible, by comparison, for the aromatic CH resonances in the 2D ^{1}H-^{13}C MAS-*J*-HMQC spectrum in Figure 3a. This is reflected in the linewidths being five times broader in the 30 kHz MAS spectrum (Figure 4) as compared to under ^{1}H FSLG decoupling (Figure 3a): the linewidths (FWHMH) for the aromatic CH (H1) SQ resonances are 1.5 ppm (730 Hz) and 0.3 ppm (170 Hz), respectively.

DQ peaks involving the NH protons are observed in Figure 4a for the intramolecular proximity between the neighboring NH and aromatic CH protons, as well as for intermolecular proximities to the aliphatic protons and notably NH−NH proximities associated with the trimer self-assembly due to intermolecular NH···N hydrogen bonding (see Figure 4b; Table S2 in the Supporting Information lists H−H distances under 3 Å for the NH as well as the aromatic CH (H1) protons in campho[2,3-c]pyrazole). The observation of the NH−NH ^{1}H DQ peak shows that fast rotation of individual molecules on their axis positions, as occurs in camphor itself, is not taking place, because the excitation and reconversion of ^{1}H DQ

TABLE 4: Spread of Experimental and Calculated (GIPAW) ^{1}H, ^{13}C, and ^{15}N Chemical Shifts for the Chemically Distinct Resonances in Campho[2,3-c]pyrazole

	$\Delta_{A-F}\delta_{iso}$ (Expt)[a]/ppm		$\Delta_{A-F}\delta_{iso}$ (Calc)/ppm			
	^{13}C/ ^{15}N	^{1}H	^{13}C/^{15}N		^{1}H	
			cryst[b]	mol[c]	cryst[b]	mol[c]
C1, H1	3.4	0.8	3.9	0.7	0.6	0.1
C3 H3	1.3	0.8	1.3	1.0	0.8	0.2
C11, H11a−c	3.4	0.5	4.3	1.7	0.7	0.3
C10, H10a−c	3.1	0.7	4.0	0.6	0.9	0.1
C8, H8a−c	2.9	1.0	3.5	0.7	1.4	0.1
C5, H5a,b	4.0	0.9	5.3	1.6	1.1	0.9
		1.1			1.3	1.3
C4, H4a,b	2.3	1.2	2.3	1.2	1.0	1.0
		1.7			1.5	1.5
C7	1.9		2.5	1.4		
C2	1.4		2.0	1.0		
C9	2.1		2.7	2.1		
C6	1.3		1.7	0.9		
NH	0.0[d]	0.0[d]	2.2	3.2	0.8	0.2
N	0.0[d]		4.6	0.8		

[a] As determined from the ^{13}C CP MAS spectrum in Figure 1b, the ^{1}H-^{13}C MAS-*J*-HMQC spectra in Figure 2, and the ^{1}H DQ MAS spectrum in Figure 4. [b] Calculation for full crystal structure, geometry-optimized with all atoms allowed to relax. [c] Calculation for isolated molecule extracted from geometry-optimized full crystal. [d] Only one resonance is resolved experimentally (for the NH ^{1}H resonance in a ^{1}H DQ MAS spectrum (see Figure 4) and for the two resonances in the ^{15}N CP MAS spectrum Figure 4a of ref 39).

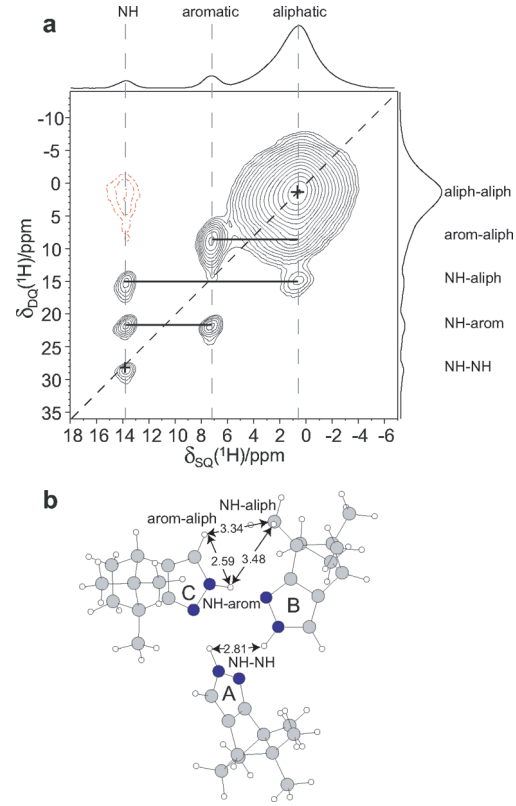

Figure 4. (a) ^{1}H (500 MHz) DQ MAS spectrum (with skyline projections) of campho[2,3-c]pyrazole recorded at 30 kHz MAS, by using one rotor period of BABA recoupling for the excitation and reconversion of DQ coherence. The base contour level is at 5%, and the $F_1 = 2F_2$ diagonal is shown as a short-dashed line. Solid horizontal bars or crosses indicate specific DQ coherences between pairs of ^{1}H nuclei. (b) Representation of the geometry-optimized (CASTEP) crystal structure showing one of the two trimers; specific H−H proximities (given in angstroms) that give rise to evident DQ peaks in (a) are identified. Note that distances corresponding to H−H proximities with the CH_3 group correspond to the distance to the CH_3 carbon atom.

coherence has been shown to be very sensitive to motion that occurs on the time scale of the experiment.[24,43,49]

For reference, Tables S3 and S4 in the Supporting Information compare the experimental and calculated (GIPAW) ^{1}H and ^{15}N chemical shifts, respectively; note that the NH ^{1}H chemical shift is determined from the ^{1}H DQ MAS spectrum in Figure 4, whereas a ^{15}N CP MAS spectrum (recorded at a ^{1}H Larmor frequency of 400 MHz) has been presented in ref 39.

3.4. Comparison of Calculated GIPAW Chemical Shifts for the Full Crystal Structure and Isolated Molecules. In Section 3.2, it was shown that the ^{13}C and ^{1}H chemical shifts that are correlated via one-bond $^{1}J_{CH}$ couplings can be assigned to the six distinct molecules in the asymmetric unit cell on the basis of GIPAW chemical-shift calculations for the full crystal structure (see Tables 1 and 2). In this section, it is shown that chemical-shift calculations can provide additional insight into the influence of intermolecular interactions on the observed chemical shifts. For example, it has been demonstrated previously that the effect of ring currents due to aromatic $\pi-\pi$ interactions or that of hydrogen bonding on solid-state chemical shifts can be quantitatively analyzed by a comparison of calculations for isolated molecules with those for small clusters of molecules in quantum-chemical calculations[58−66] or for the full crystal structure in plane-wave pseudopotential approaches.[28,67,68]

In addition to the calculated chemical shifts for the full crystal structure, Tables 1 (CH and CH_3), 2 (CH_2), and 3 (quaternary C), as well as S3 (NH) and S4 (N) in the Supporting Information, present ^{1}H, ^{13}C, and ^{15}N chemical shifts calculated for the six distinct isolated molecules as extracted from the geometry-optimized crystal structure. In Table 4, the spread in the chemical shifts over the six distinct molecules in the asymmetric unit cell for each of the four separate calculations is compared with experiment. It is evident that calculations for the individual isolated molecules (as extracted from the full crystal structure, i.e., without further geometry optimization) are insufficient to explain the experimentally observed spread of chemical shifts, showing the importance of intermolecular interactions that are considered in the calculations for the full crystal structure. (For the CH_2 ^{1}H chemical shifts, although the spread in chemical shifts is similar between the calculations for the individual isolated molecules and for the full crystal structure, an inspection of Table 2 shows that good agreement between calculation and experiment is only obtained for the full crystal structure calculation.) A listing of $\Delta\delta^{cryst-mol}$ for all calculated chemical shifts is given in Table S5 in the Supporting Information.

Figure 5 compares graphically the experimental and calculated (a) ^{13}C and (b) ^{1}H chemical shifts. Although excellent agreement is noted for calculations for the full crystal structure (black squares), poorer agreement is evident for calculations for the six isolated molecules extracted from the crystal structure (after a further geometry optimization where all atoms were allowed to relax, red circles). This is particularly evident for the isolated molecule calculated CH_3 and CH_2 ^{1}H chemical shifts, where changes of up to 2 ppm are apparent as compared to the full crystal structure calculations.

For the NH ^{1}H chemical shift, there is a large $\Delta\delta^{cryst-mol}$ equal to 5−6 ppm associated with the intermolecular NH···N hydrogen bonding (see Figure 4 and Table S5 in the Supporting Information): similar $\Delta\delta^{cryst-mol}$ values have been determined for ^{1}H chemical shifts of NH moieties in *L*-histidine·HCl·H_2O[67] and uracil[68] that exhibit intermolecular NH···O hydrogen

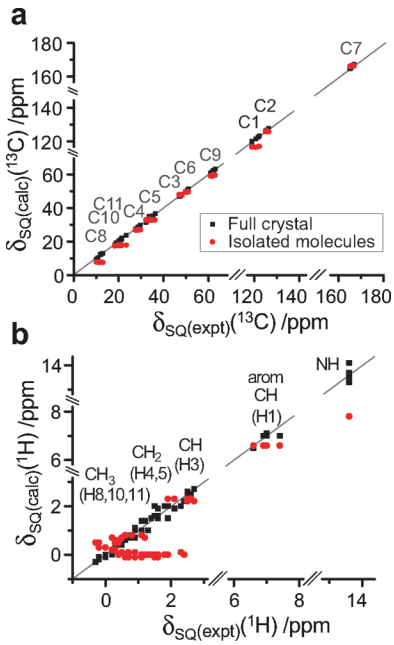

Figure 5. Comparison of experimental and calculated (GIPAW) (a) ^{13}C and (b) ^{1}H chemical shifts for campho[2,3-c]pyrazole. Black squares and red circles correspond to the chemical shifts calculated for the complete (geometry-optimized) crystal structure and those calculated for the six isolated molecules extracted from the crystal structure (after a further geometry optimization where all atoms were allowed to relax), respectively. Separate chemical-shift references, σ_{ref}, are used for each chemically distinct site (see Tables 1−3 and S3 in the Supporting Information).

bonding. An additional change of 0.5−0.7 ppm is observed in the calculated NH ^{1}H chemical shift for the isolated molecules after further geometry optimization (see Table S5 in the Supporting Information), with this change being reflected in a ~0.03 Å change in the NH bond length (from 1.046 to 1.050 Å for the six distinct molecules to 1.014 Å); similar changes in the calculated ^{1}H chemical shift and NH bond length were observed previously for uracil (see Table 1 of ref 68). By comparison, the $\Delta\delta^{cryst-mol}$ values are small (<1 ppm) for the CH ^{1}H chemical shifts, and there is no change (within 0.1 ppm) upon further geometry optimization, this being reflected in the CH bond lengths which are very similar before and after geometry optimization (within 0.002 Å: for H1, 1.084 to 1.085 Å before and 1.085 to 1.086 Å after geometry optimization; for H3, 1.096 to 1.097 Å before and 1.097 to 1.098 Å after geometry optimization).

4. Conclusions

The ^{13}C and ^{1}H resonances for the six distinct molecules in the asymmetric unit of the crystal structure of campho[2,3-c]-pyrazole have been experimentally determined by means of ^{1}H-^{13}C 2D MAS-*J*-HMQC solid-state NMR correlation spectra, and a complete assignment has been proposed for all atoms in combination with GIPAW chemical-shift calculations for the complete crystal structure, corresponding to a whole unit cell of $12 \times 29 = 348$ atoms. (Note that the assignment could in principle be confirmed with methods for tracing out the carbon−carbon backbone, e.g., the refocused INADEQUATE[69,70] and DQ-filtered COSY[71] experiments, that allow the ^{13}C resonances to be assigned to distinct molecules in the asymmetric unit cell;[32,72,73] such approaches have the disadvantage, however, that, at natural abundance in ^{13}C (1.1%), for each pair of correlation peaks, a NMR signal is only observed for ~1 in 10 000 molecules having two neighboring ^{13}C nuclei, such that long experimental times are required.)

Comparing chemical shifts calculated for isolated molecules extracted from the crystal structure with those calculated for the full crystal structure gives quantitative insight into the effect of intermolecular interactions, namely, $\pi-\pi$ interactions and hydrogen bonding, on the experimentally observed chemical shifts, in particular the spread of chemical shifts corresponding to the six distinct molecules. In conclusion, this study has demonstrated the increasing power of NMR crystallography approaches for gaining insight into the packing of organic molecules in the solid state.[35,74−77]

Acknowledgment. Funding from EPSRC (U.K.) and MEC-(CTQ2007-62113) (Spain) is acknowledged. CASTEP calculations were performed on the University of Warwick Centre for Scientific Computing cluster. We are grateful to Accelrys for providing the Materials Studio Interface. Helpful discussions with Anne Lesage and Bénédicte Elena are acknowledged.

Supporting Information Available: (i) Expanded regions for all resonances of the ^{13}C CP MAS spectrum shown in Figure 1b, (ii) calculated chemical-shift values determined by using the universal referencing values, including for the geometry-optimized extracted individual molecules, (iii) H−H distances involving CH and NH protons (cf ^{1}H DQ MAS spectrum in Figure 4), (iv) calculated and experimental ^{1}H and ^{15}N chemical shifts for the N and NH sites, (v) $\Delta\delta^{cryst-mol}$ values for the calculated ^{1}H, ^{13}C, and ^{15}N chemical shifts (pdf), and (vi) geometry-optimized (CASTEP) structures for the full crystal and extracted isolated molecules (zip of pdb files). This material is available free of charge via the Internet at http://pubs.acs.org.

References and Notes

(1) Steed, J. W. *Cryst. Eng. Comm.* **2003**, *5*, 169.
(2) Roy, S.; Banerjee, R.; Nangia, A.; Kruger, G. J. *Chem., Eur. J.* **2006**, *12*, 3777.
(3) Desiraju, G. R. *Cryst. Eng. Comm.* **2007**, *9*, 91.
(4) Anderson, K. M.; Steed, J. W. *Cryst. Eng. Comm.* **2007**, *9*, 328.
(5) Nichol, G. S.; Clegg, W. *Cryst. Eng. Comm.* **2007**, *9*, 959.
(6) Bond, A. D. *Cryst. Eng. Comm.* **2008**, *10*, 411.
(7) Bernstein, J.; Dunitz, J. D.; Gavezzotti, A. *Cryst. Growth Des.* **2008**, *8*, 2011.
(8) Anderson, K. M.; Goeta, A. E.; Steed, J. W. *Cryst. Growth Des.* **2008**, *8*, 2517.
(9) www.dur.ac.uk/zprime.
(10) Harris, R. K. *Analyst* **2006**, *131*, 351.
(11) Lesage, A.; Sakellariou, D.; Steuernagel, S.; Emsley, L. *J. Am. Chem. Soc.* **1998**, *120*, 13194.
(12) Pickard, C. J.; Mauri, F. *Phys. Rev. B* **2001**, *63*, 245101.
(13) Yates, J. R.; Pickard, C. J.; Mauri, F. *Phys. Rev. B* **2007**, *76*, 024401.
(14) Madhu, P. K. *Solid State Nucl. Magn. Reson.* **2009**, *35*, 2.
(15) Bielecki, A.; Kolbert, A. C.; Levitt, M. H. *Chem. Phys. Lett.* **1989**, *155*, 341.
(16) Vinogradov, E.; Madhu, P. K.; Vega, S. *Chem. Phys. Lett.* **1999**, *314*, 443.
(17) Sakellariou, D.; Lesage, A.; Hodgkinson, P.; Emsley, L. *Chem. Phys. Lett.* **2000**, *319*, 253.
(18) Lesage, A.; Sakellariou, D.; Hediger, S.; Elena, B.; Charmont, P.; Steuernagel, S.; Emsley, L. *J. Magn. Reson.* **2003**, *163*, 105.
(19) Elena, B.; de Paepe, G.; Emsley, L. *Chem. Phys. Lett.* **2004**, *398*, 532.
(20) Salager, E.; Stein, R. S.; Steuernagel, S.; Lesage, A.; Elena, B.; Emsley, L. *Chem. Phys. Lett.* **2009**, *469*, 336.
(21) Elena, B.; Lesage, A.; Steuernagel, S.; Bockmann, A.; Emsley, L. *J. Am. Chem. Soc.* **2005**, *127*, 17296.
(22) Brown, S. P.; Spiess, H. W. *Chem. Rev.* **2001**, *101*, 4125.
(23) Lesage, A. *Phys. Chem. Chem. Phys.* **2009**, *11*, 6876.
(24) Brown, S. P. *Macromol. Rapid Commun.* **2009**, *30*, 688.
(25) Harris, R. K.; Hodgkinson, P.; Pickard, C. J.; Yates, J. R.; Zorin, V. *Magn. Reson. Chem.* **2007**, *45*, S174.
(26) www.gipaw.net.

(27) Yates, J. R.; Dobbins, S. E.; Pickard, C. J.; Mauri, F.; Ghi, P. Y.; Harris, R. K. *Phys. Chem. Chem. Phys.* **2005**, *7*, 1402.
(28) Yates, J. R.; Pham, T. N.; Pickard, C. J.; Mauri, F.; Amado, A. M.; Gil, A. M.; Brown, S. P. *J. Am. Chem. Soc.* **2005**, *127*, 10216.
(29) Gervais, C.; Dupree, R.; Pike, K. J.; Bonhomme, C.; Profeta, M.; Pickard, C. J.; Mauri, F. *J. Phys. Chem. A* **2005**, *109*, 6960.
(30) Mifsud, N.; Elena, B.; Pickard, C. J.; Lesage, A.; Emsley, L. *Phys. Chem. Chem. Phys.* **2006**, *8*, 3418.
(31) Shao, L. M.; Yates, J. R.; Titman, J. J. *J. Phys. Chem. A* **2007**, *111*, 13126.
(32) Harris, R. K.; Cadars, S.; Emsley, L.; Yates, J. R.; Pickard, C. J.; Jetti, R. K. R.; Griesser, U. J. *Phys. Chem. Chem. Phys.* **2007**, *9*, 360.
(33) Zurek, E.; Pickard, C. J.; Autschbach, J. *J. Am. Chem. Soc.* **2007**, *129*, 4430.
(34) Johnston, J. C.; Iuliucci, R. J.; Facelli, J. C.; Fitzgerald, G.; Mueller, K. T. *J. Chem. Phys.* **2009**, *131*, 144503.
(35) Salager, E.; Day, G. M.; Stein, R. S.; Pickard, C. J.; Elena, B.; Emsley, L. *J. Am. Chem. Soc.* **2010**, *132*, 2564.
(36) Milman, V.; Refson, K.; Clark, S. J.; Pickard, C. J.; Yates, J. R.; Gao, S.-P.; Hasnip, P. J.; Probert, M. J.; Perlov, A.; Segall, M. D. *J. Mol. Struct. THEOCHEM* **2010**, *954*, 22.
(37) Jacquier, R.; Maury, G. *Bull. Soc. Chim. Fr.* **1967**, 295.
(38) Llamas-Saiz, A. L.; Foces-Foces, C.; Sobrados, I.; Elguero, J.; Meutermans, W. *Acta Crystallogr. C* **1993**, *49*, 724.
(39) Yap, G. P. A.; Claramunt, R. M.; López, C.; Garcia, M. A.; Pérez-Medina, C.; Alkorta, I.; Elguero, J. *J. Mol. Struct.* **2010**, *965*, 74.
(40) Hediger, S.; Meier, B. H.; Kurur, N. D.; Bodenhausen, G.; Ernst, R. R. *Chem. Phys. Lett.* **1994**, *223*, 283.
(41) Metz, G.; Wu, X. L.; Smith, S. O. *J. Magn. Reson. Ser. A* **1994**, *110*, 219.
(42) Bennett, A. E.; Rienstra, C. M.; Auger, M.; Lakshmi, K. V.; Griffin, R. G. *J. Chem. Phys.* **1995**, *103*, 6951.
(43) Brown, S. P. *Prog. Nucl. Magn. Reson. Spectrosc.* **2007**, *50*, 199.
(44) Sommer, W.; Gottwald, J.; Demco, D. E.; Spiess, H. W. *J. Magn. Reson. Ser. A* **1995**, *113*, 131.
(45) Schnell, I.; Lupulescu, A.; Hafner, S.; Demco, D. E.; Spiess, H. W. *J. Magn. Reson.* **1998**, *133*, 61.
(46) Clark, S. J.; Segall, M. D.; Pickard, C. J.; Hasnip, P. J.; Probert, M. J.; Refson, K.; Payne, M. C. *Z. Kristallogr.* **2005**, *220*, 567.
(47) Perdew, J. P.; Burke, K.; Enzernhof, M. *Phys. Rev. Lett.* **1999**, *77*, 3865.
(48) Vanderbilt, D. *Phys. Rev. B* **1990**, *41*, 7892.
(49) Brown, S. P.; Schnell, I.; Brand, J. D.; Mullen, K.; Spiess, H. W. *Phys. Chem. Chem. Phys.* **2000**, *2*, 1735.
(50) Brown, S. P.; Zhu, X. X.; Saalwachter, K.; Spiess, H. W. *J. Am. Chem. Soc.* **2001**, *123*, 4275.
(51) Pickard, C. J.; Salager, E.; Pintacuda, G.; Elena, B.; Emsley, L. *J. Am. Chem. Soc.* **2007**, *129*, 8932.
(52) Webber, A. L.; Elena, B.; Griffin, J. M.; Yates, J. R.; Pham, T. N.; Mauri, F.; Pickard, C. J.; Gil, A. M.; Stein, R.; Lesage, A.; Emsley, L.; Brown, S. P. *Phys. Chem. Chem. Phys.* **2010**, *12*, 6970.
(53) Dumez, J. N.; Pickard, C. J. *J. Chem. Phys.* **2009**, *130*, 104701.
(54) Rossano, S.; Mauri, F.; Pickard, C. J.; Farnan, I. *J. Phys. Chem. B* **2005**, *109*, 7245.
(55) De Gortari, I.; Portella, G.; Salvatella, X.; Bajaj, V. S.; van der Wel, P. C. A.; Yates, J. R.; Segall, M. D.; Pickard, C. J.; Payne, M. C.; Vendruscolo, M. *J. Am. Chem. Soc.* **2010**, *132*, 5993.
(56) Hansen, M. R.; Graf, R.; Sekharan, S.; Sebastiani, D. *J. Am. Chem. Soc.* **2009**, *131*, 5251.
(57) Harris, R. K.; Hodgkinson, P.; Larsson, T.; Muruganantham, A.; Ymen, I.; Yufit, D. S.; Zorin, V. *Cryst. Growth Des.* **2008**, *8*, 80.
(58) Ochsenfeld, C.; Brown, S. P.; Schnell, I.; Gauss, J.; Spiess, H. W. *J. Am. Chem. Soc.* **2001**, *123*, 2597.
(59) Brown, S. P.; Schaller, T.; Seelbach, U. P.; Koziol, F.; Ochsenfeld, C.; Klarner, F. G.; Spiess, H. W. *Angew. Chem., Int. Edit.* **2001**, *40*, 717.
(60) Ochsenfeld, C.; Koziol, F.; Brown, S. P.; Schaller, T.; Seelbach, U. P.; Klarner, F. G. *Solid State Nucl. Magn. Reson.* **2002**, *22*, 128.
(61) Harris, R. K.; Ghi, P. Y.; Hammond, R. B.; Ma, C. Y.; Roberts, K. J. *Chem. Commun.* **2003**, 2834.
(62) Heine, T.; Corminboeuf, C.; Grossmann, G.; Haeberlen, U. *Angew. Chem., Int. Edit.* **2006**, *45*, 7292.
(63) Brouwer, D. H.; Alavi, S.; Ripmeester, J. A. *Phys. Chem. Chem. Phys.* **2008**, *10*, 3857.
(64) Metzroth, T.; Lenhart, M.; Gauss, J. *Appl. Magn. Reson.* **2008**, *33*, 457.
(65) Wu, G. *Prog. Nucl. Magn. Reson. Spectrosc.* **2008**, *52*, 118.
(66) Schaller, T.; Buchele, U. P.; Klarner, F. G.; Blaser, D.; Boese, R.; Brown, S. P.; Spiess, H. W.; Koziol, F.; Kussmann, J.; Ochsenfeld, C. *J. Am. Chem. Soc.* **2007**, *129*, 1293.
(67) Schmidt, J.; Hoffmann, A.; Spiess, H. W.; Sebastiani, D. *J. Phys. Chem. B* **2006**, *110*, 23204.
(68) Uldry, A. C.; Griffin, J. M.; Yates, J. R.; Perez-Torralba, M.; Maria, M. D. S.; Webber, A. L.; Beaumont, M. L. L.; Samoson, A.; Claramunt, R. M.; Pickard, C. J.; Brown, S. P. *J. Am. Chem. Soc.* **2008**, *130*, 945.
(69) Lesage, A.; Bardet, M.; Emsley, L. *J. Am. Chem. Soc.* **1999**, *121*, 10987.
(70) Fayon, F.; Massiot, D.; Levitt, M. H.; Titman, J. J.; Gregory, D. H.; Duma, L.; Emsley, L.; Brown, S. P. *J. Chem. Phys.* **2005**, *122*, 194313.
(71) Lee, D.; Struppe, J.; Elliott, D. W.; Mueller, L. J.; Titman, J. J. *Phys. Chem. Chem. Phys.* **2009**, *11*, 3547.
(72) Olsen, R. A.; Struppe, J.; Elliott, D. W.; Thomas, R. J.; Mueller, L. J. *J. Am. Chem. Soc.* **2003**, *125*, 11784.
(73) Harris, R. K.; Joyce, S. A.; Pickard, C. J.; Cadars, S.; Emsley, L. *Phys. Chem. Chem. Phys.* **2006**, *8*, 137.
(74) Harris, R. K. *Solid State Sci.* **2004**, *6*, 1025.
(75) Taulelle, F. *Solid State Sci.* **2004**, *6*, 1053.
(76) Elena, B.; Pintacuda, G.; Mifsud, N.; Emsley, L. *J. Am. Chem. Soc.* **2006**, *128*, 9555.
(77) Harris, R. K., Wasylishen, R. E., Duer, M. J., Eds.; *NMR Crystallography*; Wiley: Chichester, 2009.

JP104901J